

A Statistical Study on Force-Freeness of Solar Magnetic Fields in the Photosphere

S. Liu¹, J.T. Su¹, H.Q. Zhang¹, Y.Y. Deng¹, Y. Gao¹, X. Yang¹, X.J. Mao^{1,2}

¹National Astronomical Observatory and key Laboratory of Solar Activity,
Chinese Academy of Sciences, Beijing 100012, China

²Department of Astronomy, Beijing Normal University, Beijing 100875, China

lius@nao.cas.cn

Received _____; accepted _____

ABSTRACT

It is an indisputable fact that solar magnetic fields are force-free in the corona, where force free fields means that current and magnetic fields are parallel and there is no Lorentz force in the fields. While the force-free extent of photospheric magnetic fields remains open. In this paper, the statistical results about it is given. The vector magnetograms (namely, B_x , B_y and B_z in heliocentric coordinates) are employed, which are deduced and calibrated from Stokes spectra, observed by Solar Magnetic Field Telescope (SMFT) at Huairou Solar Observing Station (HSOS) are used. We study and calibrated 925 magnetograms calibrated by two sets of calibration coefficients, that indicate the relations between magnetic fields and the strength of Stokes spectrum and can be calculated either theoretically or empirically. The statistical results show that the majority of active region magnetic fields are not consistent with the force-free model.

Subject headings: Magnetic field, Photosphere, Corona

1. Introduction

Magnetic fields dominate most solar activities such as filaments eruption, flares and coronal mass ejections (CMEs). All these phenomena are energetic events due to explosive release of magnetic energy (Krall et al. 1982; Shibata et al. 1995; Tsuneta 1996; Wan 1994; Bond et al. 2001; Priest & Forbes 2003; Nindos 2012). Thus the solar magnetic field is the key for us to understand the nature of solar activities. Since the measurable magnetic sensitive lines are around the photosphere, the reliable measurements of magnetic fields are nearly there (Stenflo 1973; Harvey 1977). However the understanding of the magnetic field in the chromosphere and corona remains difficult due to both intrinsic physical difficulties and observational limitations (Gary & Hurford 1994; Lin et al. 2004). Generally, magnetic fields in the corona are regarded as a force-free (Aly 1989), because the plasma β (ratio of plasma pressure to magnetic pressure over there) is much less than unity. But it is controversial in the photosphere, because two kinds of pressure are comparable (Demoulin et al. 1997). For the low- β corona where the plasma is tenuous ($\beta \ll 1$), magnetic field satisfies the following force-free equations:

$$\nabla \times \mathbf{B} = \alpha(\mathbf{r})\mathbf{B}, \quad (1)$$

$$\nabla \cdot \mathbf{B} = 0. \quad (2)$$

They imply that there is no Lorentz force in action and α is constant along magnetic field lines ($\mathbf{B} \cdot \nabla \alpha = 0$).

At present, the magnetic field extrapolation with a force-free assumption is a major method to study the solar magnetic fields of active regions. The coronal fields can be reconstructed from a physical model (namely, force free model) in which the observed photospheric magnetic field is taken as a boundary condition (Wu et al. 1990; Mikic et al. 1994; Amari et al. 1997; Sakurai 1981; Yan & Sakurai 2000; Wheatland et al. 2000; Wiegelmann 2004; Song et al. 2006; He & Wang 2008; Liu et al. 2011). It means that coronal magnetic fields are considered to be

force-free, while at the boundary it is connected to the photospheric magnetic fields observed. The force-free extent of the photospheric magnetic field then becomes an important subject to study. Wiegmann et al. (2006) proposed a preprocessing procedure to make a minor regulation within the allowable errors, so that the observed magnetic fields are biased to a force-free, which further indicates the study of force-free extent is significant and necessary for the field extrapolation. Metcalf et al. (1995) calculated dependence of the net Lorentz force in the photosphere and low chromosphere on the height using Mees Solar Observatory magnetograms and concluded that the magnetic fields are not force free in the photosphere, but becomes force-free roughly 400 km above the photosphere. Moon et al. (2002) studying the force-free extent in the photosphere using 12 vector magnetograms of three active regions, realized that the photospheric magnetic fields are not very far from the force-free case. Liu et al. (2011) tentatively applied the force-free extrapolation to reconstruct the magnetic fields above the quiet region and checked the force-free extent of this quiet region based on the high spatial resolution vector magnetograms observed by the Solar Optical Telescope/Spectro-Polarimeter on board Hinode. Tiwari (2012) found sunspot magnetic fields are not so far from the force-free. We, in this paper, conduct a the statistical research to make use of the vector magnetograms observed by SMFT at HSOS from 1988 to 2001 in order to verify the force-freeness of the photospheric magnetic field.

The paper is organized as follows: firstly, the description of observations and data reduction is arranged in Section 2; then, the results are shown in Section 3; finally, in section 4 presents the short discussions and conclusions.

2. Observations and Data Reduction

The observational data used here are 925 vector magnetograms corresponding to 925 active regions observed from 1988 to 2001 by solar Magnetic Field Telescope (SMFT) installed at Huairou Solar Observing Station (HSOS), located at north shore of Huairou reservoir.

Magnetograms associated with the corresponding to the active region, which is the nearest to disk center is chosen and calculated. So only one magnetogram is available for one active region. SMFT consists of 35 cm refractor with a vacuum tube, birefringent filter, CCD camera including an image processing system operated by computer (Ai & Hu 1986). The birefringent filter is tunable, working either at the photosphere line Fe I λ 5324.19 Å, with a 0.150 Å bandpass, or at the chromosphere line, H β , with a 0.125 Å bandpass. The line of Fe I λ 5324.19 Å (Lande factor $g = 1.5$) formed around the solar photosphere, is used for photospheric magnetic field observations. The bandpass of the birefringent filter is about 0.15 Å for Fe I λ 5324.19 Å line. The center wavelength of the filter can normally be shifted -0.075 Å relative to center of Fe I λ 5324.19 Å to measure of the longitudinal magnetic field and then the line center is applied to measure the transverse one (Ai & Hu 1986). Vector magnetograms are reconstructed from four narrow-band images of Stokes parameters (I , Q , U and V). V is the difference of the left and right circularly polarized images, Q and U are the differences between two orthogonal linearly polarized images for different azimuthal directions, I is the intensity derived from either the sum of two circularly polarized images is the line-of-sight field measurements or of two linearly polarized images in the transverse field measurement. When I , Q , U and V are measured, the corresponding white light images are simultaneously obtained, which are employed to compensate for the time differences during the measurements of I , Q , U and V . The sequence of obtaining Stokes images is as follows: First acquired the V/I image ; next the Q/I images, then the U/I image. The time required to obtain a set of Stokes images was about 45 second. Each image is associated with 256 integrated frames. To reconstruct the vector magnetograms, the linear relation is necessary between the magnetic field and the Stokes parameters I , Q , U and V , which is true under the weak-field approximation (Jefferies et al. 1989; Jefferies & Mickey 1991):

$$B_L = C_L V, \quad (3)$$

$$B_T = C_T (Q^2 + U^2)^{1/4}, \quad (4)$$

$$\theta = \arctan\left(\frac{B_L}{B_\perp}\right), \quad (5)$$

$$\phi = \frac{1}{2}\arctan\left(\frac{U}{Q}\right), \quad (6)$$

where B_L and B_T are the line-of-sight and transverse component of the photospheric field, respectively. θ is the inclination between the vector magnetic field and the direction normal to the solar surface and ϕ is the field azimuth. C_L and C_T are the calibration coefficients for the longitudinal and transverse magnetic fields, respectively. Both theoretical and empirical methods are used to calibrate vector magnetograms (Wang, Ai & Deng 1996; Ai et al. 1982). So that two sets of calibration coefficients are available: the first set C_L and C_T are 8381 G and 6790 G (Su & Zhang 2004; Wang, Ai & Deng 1996), respectively, obtained by theoretical calibration; in the second set C_L and C_T are 10000 G and 9730 G, respectively, which are deduced through empirical calibrations (Wang et al. 1996). Faraday rotation and magneto optical effects may affect the value of measured magnetic fields. Bao et al. (2000) analyzed the Faraday rotation in the HSOS magnetograms which contributes about 12° . Gao et al. (2008) proposed a way of the statistical removal of Faraday rotation in vector magnetograms from HSOS. Zhang (2000) found that the statistical mean azimuth error of the transverse field is 12.8° caused by magneto optical effects. In addition, there may be other causes of the data uncertainty. For example, saturation effects, filling factors and stray light. After routine data processing of HSOS data, the spatial resolution of observational data is actually $2 \text{ arcsec/pixel} \times 2 \text{ arcsec/pixel}$ and 3σ noise levels of vector magnetograms are 20 G and 150 G for longitudinal and transverse components, respectively.

The acute angle method is employed to resolve 180° ambiguity (Wang, Zhang & Ai 1994; Wang 1997; Wang, Yan & Sakurai 2001; Metcalf et al. 2006), in which the observed field is compared to the extrapolated potential field in the photosphere. The orientation of the observed transverse component is chosen by requiring $-90^\circ \leq \Delta\theta \leq 90^\circ$, where $\Delta\theta = \theta_o - \theta_e$ is the angle difference between the observed and extrapolated transverse components. At last, the components

of the vector magnetic field ($B_x = B_T \cos\phi$, $B_y = B_T \sin\phi$ ($B_T = \sqrt{B_x^2 + B_y^2}$) and $B_z = B_L \cos\theta$) are calculated in local heliocentric coordinates. To minimize the projection effects, the requirement that the horizontal width of an active region is less than 20 degree is added for each magnetogram.

3. Results

In classical electromagnetic theory, Lorentz force can be written as the divergence of the Maxwell stress:

$$\mathbf{F} = \frac{(\mathbf{B} \cdot \nabla)\mathbf{B}}{4\pi} - \frac{\nabla(\mathbf{B} \cdot \mathbf{B})}{8\pi}, \quad (7)$$

Under the assumption that the magnetic field above the plane $z = 0$ (namely, the photosphere) falls off fast enough as going to infinity, the net Lorentz force in the infinite half-space $z > 0$ is just the Maxwell stress integrated over the plane $z = 0$ (Chandrasekhar 1961; Molodensky 1974; Aly 1984; Low 1985). Then, the components of the net Lorentz force at the plane $z = 0$ can be expressed by the surface integrals as follows:

$$F_x = -\frac{1}{4\pi} \int B_x B_z dx dy, \quad (8)$$

$$F_y = -\frac{1}{4\pi} \int B_y B_z dx dy, \quad (9)$$

$$F_z = -\frac{1}{8\pi} \int (B_z^2 - B_x^2 - B_y^2) dx dy. \quad (10)$$

The necessary conditions of a force-free field are that all three components are much less than F_p (Low 1985), where F_p is a characteristic magnitude of the total Lorentz force and can be written as:

$$F_p = \frac{1}{8\pi} \int (B_z^2 + B_x^2 + B_y^2) dx dy, \quad (11)$$

The values of F_x/F_p , F_y/F_p , and F_z/F_p then provide a measure of the force-free extent at the boundary plane $z = 0$ (the photosphere).

Following Metcalf et al. (1995) and Moon et al. (2002), F_x/F_p , F_y/F_p , and F_z/F_p are utilized to check the force-free extent of the selected photospheric magnetograms. The necessary conditions of the force-free field are also expressed as: $|F_x|/F_p \ll 1$, $|F_y|/F_p \ll 1$, and $|F_z|/F_p \ll 1$ (Metcalf et al. 1995; Moon et al. 2002), that is if three parameters F_x/F_p , F_y/F_p and F_z/F_p are so small that they are negligible then the magnetic field can be regarded as a force-free completely. Metcalf et al. (1995) suggested that the magnetic field is a force-free if the F_z/F_p is less than or equal to 0.1. The calibration coefficients C_L and C_T may affect the three parameters of F_x/F_p , F_y/F_p and F_z/F_p . Thus, two sets of calibration coefficients mentioned above are applied to this study. CaseI: C_L and C_T are chosen as 8381 G and 6790 G (Su & Zhang 2004; Wang, Ai & Deng 1996), respectively. CaseII: C_L and C_T are chosen as 10000 G and 9730 G (Wang et al. 1996), respectively.

Fig 1 shows the possibility density function (PDF) and scatter diagrams of F_x/F_p , F_y/F_p and F_z/F_p for the selected magnetograms (CaseI). The mean values of absolute F_x/F_p , F_y/F_p and F_z/F_p for all selected 925 magnetograms are 0.077, 0.109 and 0.302, respectively. The amplitudes of F_x/F_p and F_y/F_p are evidently smaller than that of F_z/F_p , which is the same as previous study (Metcalf et al. 1995). Therefore F_z/F_p can work as a criterion indicating a force-free or non-force-free field more evidently. From the distributions of PDF and scatter diagrams, the most of magnetograms have the amplitudes of F_z/F_p distributed outside the zone consisting the width of ± 0.1 , which means the most of the photospheric magnetic fields deviate from a force-free field. There are about 17% of the magnetograms with the values of F_z/F_p less than 0.1 for CaseI (38% of the magnetograms with the values of F_z/F_p less than 0.2). To see the relation between F_x/F_p , F_y/F_p and F_z/F_p and magnetic field strength, Fig 2 shows F_x/F_p , F_y/F_p and F_z/F_p vs the magnetic components of B_x , B_y and B_z for the selected magnetograms (CaseI), where B_x , B_y and B_z are the average of the absolute values of all pixels for each magnetogram. It can be seen only at the bottom right of Fig 2 that the amplitudes of F_z/F_p decrease roughly as B_z increase, and there is no evident correlations exist between the parameters (F_x/F_p , F_y/F_p or F_z/F_p) and magnetic

components, but according to Equation (10), the value of F_z/F_p should decrease as B_z increasing.

To study the effect of calibration coefficients on these three parameters of F_x/F_p , F_y/F_p and F_z/F_p , PDF and scatter diagrams of F_x/F_p , F_y/F_p and F_z/F_p of the selected magnetograms (CaseII) are plotted in Fig 5. the amplitudes of F_x/F_p and F_y/F_p same as CaseI are smaller than that of F_z/F_p evidently. For CaseII, The mean values of absolute F_x/F_p , F_y/F_p and F_z/F_p for all selected magnetograms are 0.078, 0.111 and 0.251, respectively, which are smaller than those of CaseI on the whole. And also for CaseII there are about 25% of the magnetograms with the value of F_z/F_p less than 0.1 (49% of the magnetograms with the values of F_z/F_p less than 0.2). It should be noted that even more F_z/F_p in the zone mentioned above (consisting the width of ± 0.1), most of magnetograms can not be regarded as a force-free. Besides, the widths of PDF are not narrow and the scatter of diagrams are diverge as well. In general, there is deviation of F_z/F_p from the zone. For CaseII, F_x/F_p , F_y/F_p , F_z/F_p and magnetic components of vs B_x , B_y and B_z are also plotted in Fig 4 to study their relations with the magnetic field strength. The results is consistent with that of CaseI, only the the amplitudes of F_z/F_p decrease as B_z increasing.

To see the differences of results of F_x/F_p , F_y/F_p and F_z/F_p between two cases, the scatter plots of F_x/F_p , F_y/F_p and F_z/F_p of CaseI vs the corresponding ones from CaseII are shown in Fig 5. The correlations are calculated, which are 0.994, 0.995 and 0.980 for F_x/F_p , F_y/F_p and F_z/F_p , respectively. Also the linear fits ($y = Ax + B$) are done based on these scatter plots, the values of A are 0.0008, 0.0003 and 0.2034 and B 1.10, 1.10 and 0.95 for F_x/F_p , F_y/F_p and F_z/F_p , respectively. The correlation show there exists high consistence between these two cases. Nevertheless correlation of F_z/F_p between two cases is not so good as those of F_x/F_p and F_y/F_p . This may imply that the more attentions should be focused on the amplitude of F_z/F_p in order to understand the extent of force-free.

4. Discussions and Conclusions

It is worth to study the force-free extent of the photospheric magnetic field while together with the case of magnetic field extrapolation, since it has been assumed that the coronal magnetic field is force-free and the photospheric one should be matched observationally. In this paper the results of force-free extent of the photospheric magnetic field are given through a statistical research, using 925 magnetograms corresponding to 925 active regions observed by SMFT at HSOS.

A part of efforts to avoid the uncertainty of the data calibration is the employment of two sets of calibration coefficients to describe the force-free extent of the photospheric magnetic field. For the caseI, the calibration coefficients C_L and C_T are 8381 G and 6790 G, the mean values of absolute F_x/F_p , F_y/F_p and F_z/F_p for all selected magnetograms are 0.077, 0.109 and 0.302, respectively, and for the caseII C_L and C_T are 10000 G and 9730 G, the mean values of absolute F_x/F_p , F_y/F_p and F_z/F_p are 0.078, 0.111 and 0.251, respectively. There are 17% and 25% magnetograms with their value of F_z/F_p less than 0.1 for caseI and caseII, respectively, in other word, 17% of caseI and 25% of caseII are force-free. Although there are differences between two cases, between them the correlation are as high as 0.994, 0.995 and 0.980, for F_x/F_p , F_y/F_p and F_z/F_p , respectively. Consequently we concluded that large part of the photospheric magnetic fields do not belong to a force-free. So before extrapolating a magnetic field, the force-free extent of the photospheric magnetic field should be adequately considered. We note that F_z/F_p decrease with the increase of B_z , which is a more important parameter indicating whether a magnetic field is force-free or not, since the amplitude of F_z/F_p is larger than those of F_x/F_p and F_y/F_p . From Equation (10), it can be seen that F_z/F_p may be neglected when the amplitude of B_z is comparable to $\sqrt{B_x^2 + B_y^2}$, while they are apparently different between B_z and $\sqrt{B_x^2 + B_y^2}$, then the amplitude of F_z/F_p should be enlarged. According to the Equations (8-(10) and observatories as well, the correlations between F_x/F_p , F_y/F_p and magnetic field component are not evident.

The strengths of active region magnetic fields observed by SMFT at HSOS are determined through calibration, under the conditions of a weak-field approximation and the linear relations between the magnetic field and the Stokes parameters I , Q , U and V . Additionally, comparing the recent data obtained from space satellite, the data of SMFT at HSOS has lower resolution and more uncertainty of magnetic amplitudes. These disadvantages may affect the statistical results we have acquired. However the statistical analysis associated with its results may have an significance as a practical reference, because SMFT has observed photospheric magnetic fields more than one solar cycles at HSOS and its reliability observations been studied strictly and adequately. It is hoped that the statistical results can be obtained based on high resolution data in the future.

The authors wish to thank the anonymous referee for his/her helpful comments and suggestions. This work was partly supported by the National Natural Science Foundation of China (Grant Nos. 10611120338, 10673016, 10733020, 10778723, 11003025, 11103037, 10878016 and 11178016), National Basic Research Program of China (Grant No. 2011CB8114001), Important Directional Projects of Chinese Academy of Sciences (Grant No. KLCX2-YW-T04), the Young Researcher Grant of National Astronomical Observatories, Chinese Academy of Sciences, and Key laboratory of Solar Activity National Astronomical Observations, Chinese Academy of Sciences.

REFERENCES

- Ai, G. & Hu, Y.: 1986, *Acta Astron. Sinica*, **27**, 173,
- Ai, G. Li, W. & Zhang, H.Q.: 1982, *Acta Astron. Sinica*, **23**, 39,
- Aly, J.J.: 1984, *ApJ* **283**, 349.
- Aly, J.J.: 1989, *Sol. Phys.* **120**, 19.
- Amari, T., Aly, J.J., Luciani, J.F., Boulmezaoud, T.Z., Mikic, Z.: 1997, *Sol. Phys.* **174**, 129.
- Bao, S. D., Pevtsov, A. A., Wang, T. J., and Zhang, H. Q.: 2000, *Sol. Phys.* **195**, 75
- Bond, H. E., Mullan, D. J., O'Brien, M. S., & Sion, E. M.: 2001, *ApJ* **560**, 919
- Chandrasekhar, S.: 1961, *Hydrodynamic and hydromagnetic stability*, chapter 13
- Gary, D. E. & Hurford, G. J.: 1994, *ApJ* **420**, 903
- Harvey, J. W.: 1977, *HighlightsofAstronomy* **4**, 223
- Gao, Y. Su, J.T., Xu, H.Q. & Zhang, H.Q.: 2008, *MNRAS* **386**, 1959
- Gary, G.A. & Hagyard, M. J.: 1990, *Sol. Phys.* **126**, 21
- He, H., Wang, H.: 2008, *J. Geophys. Res.* **113**, A05S90
- Jefferies, J., Lites, B.W. & Skumanich, A.: 1989, *ApJ* **343**, 920
- Jefferies, J., & Mickey, D.L.: 1991, *ApJ* **372**, 694
- Krall, K. R., Smith, J. B., Jr., Hagyard, M. J., West, E. A. & Cummings, N. P.: 1982, *Sol. Phys.* **79**, 59
- Lin, J., Y.-K. Ko, Sui, L., Raymond, J.C., Stenborg, G.A., Jiang, Y., Zhao, S. & Mancuso, S.: 2005, *ApJ* **622**, 1251

Lin,S., Zhang, H.Q. & Su, J.T.: 2011, Sol. Phys. **270**, 89

Lin,S., Zhang, H.Q., Su, J.T. & Song, M.T.: 2011, Sol. Phys. **269**, 41

Liu, H., Kuhn, J.R. & Coulter, R.:

Low, B.C.: 1984, in Measurements of Solar Vector Magnetic Fields, Vol. 2374, ed. M. J. Hagyard
(Washington, DC: NASA), 49

Demoulin, P., Bagala, L. G., Mandrini, C. H., Henoux, J. C., & Rovira, . G.: 1997, A&A, 256, 305

Metcalf, T. R., Leka, K. D., Barnes, G., Lites, B. W., Georgoulis, M. K., Pevtsov, A. A.,
Balasubramaniam, K. S., Gary, G. A., Jing, J., & Li, J.: 2006, Sol. Phys. **237**, 267.

Metcalf, T. R., Jiao, L., McClymont, A. N., Canfield, R. C., & Uitenbroek, H.: 1995, ApJ **439**,
474

Mikic, Z.; McClymont, A. N.: 1994, in Solar Active Region Evolution: Comparing Models with
Observations, Vol68. ASP Conf. Ser., p.225.

Molodensky, M. M.: 1974, Sol. Phys. **39**, 393

Moon, Y., Choe, G. S., Yun, H. S., Park, Y. D., & Mickey, D. L.: 2002, ApJ **568**, 422

Nindos, A., Patsourakos, S. & Wiegmann, T. 2012, ApJ, **748**, L6

Priest, E.R. & Forbes, T.G.: 2002, *Astron. Astrophys. Rev.* **10**, 313

Sakurai, T.: 1981, Sol. Phys. **69**, 343.

Shibata, K., S. Masuda, M. Shimojo, H. Hara, T. Yokoyama, S. Tsuneta, T. Kosugi, & Y. Ogawara:
1995, ApJ. **451**, L83

Song, M.T., Fang, C., Tang, Y.H., Wu, S.T., Zhang, Y.A.: 2006, ApJ **649**, 1084.

- Stenflo, J.O.: 1973, *Sol. Phys.* **32**, 41
- Su, J.T. & Zhang, H.Q.: 2004, *Chin. J. Astron. Astrophys.* **4**, 365
- Tiwari, S.K.: 2012, *ApJ* **744**, 65
- Tsuneta, S.: 1996, *ApJ* **456**, 840
- Wang, H.: 1997, *Sol. Phys.* **174**, 265.
- Wang, H., Ewell, M. W., Jr., Zirin, H. & Ai, G.X.: 1994, *ApJ* **424**, 436.
- Wang, H., Yan, Y., & Sakurai, T.: 2001, *Sol. Phys.* **201**, 323.
- Wang, J.X., Shi, Z.X., Wang, H.N. & Lu, Y.P.: 1996, *ApJ* **456**, 861.
- Wang T.J., Ai G.X., Deng, Y.Y.: 1996, *Astrophysics Reports.*, **23**, 31
- Wang, T., Zhang, H. and Xu, A.: 1994, *Sol. Phys.* **155**, 99.
- Wheatland, M.S., Sturrock, P.A., Roumeliotis, G.: 2000, *ApJ* **540**, 1150.
- Wiegelmann, T.: 2004, *Sol. Phys.* **219**, 87.
- Wiegelmann, T., Inhester, B., & Sakurai, T.: 2006, *Sol. Phys.* **233**, 215.
- Wu, S.T., Sun, M.T., Chang, H.M., Hagyard, M.J., Gary, G.A.: 1990, *ApJ* **362**, 698.
- Yan, Y., Sakurai, T.: 2000, *Sol. Phys.* **195**, 89.
- Zhang, H.Q.: 2000, *Sol. Phys.* **197**, 235.

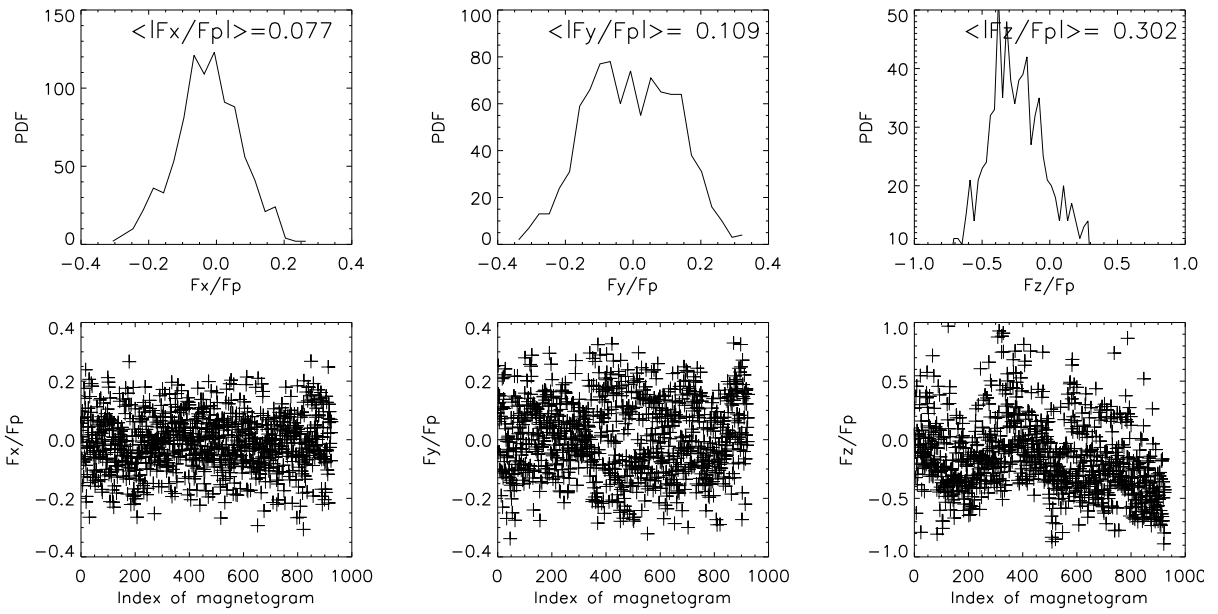


Fig. 1.— PDF and scatter diagrams of F_x/F_p , F_y/F_p and F_z/F_p for the selected magnetograms. The mean values of absolute F_x/F_p , F_y/F_p and F_z/F_p are plotted and indicated by $\langle |F_x/F_p| \rangle$, $\langle |F_y/F_p| \rangle$, $\langle |F_z/F_p| \rangle$, respectively. (CaseI)

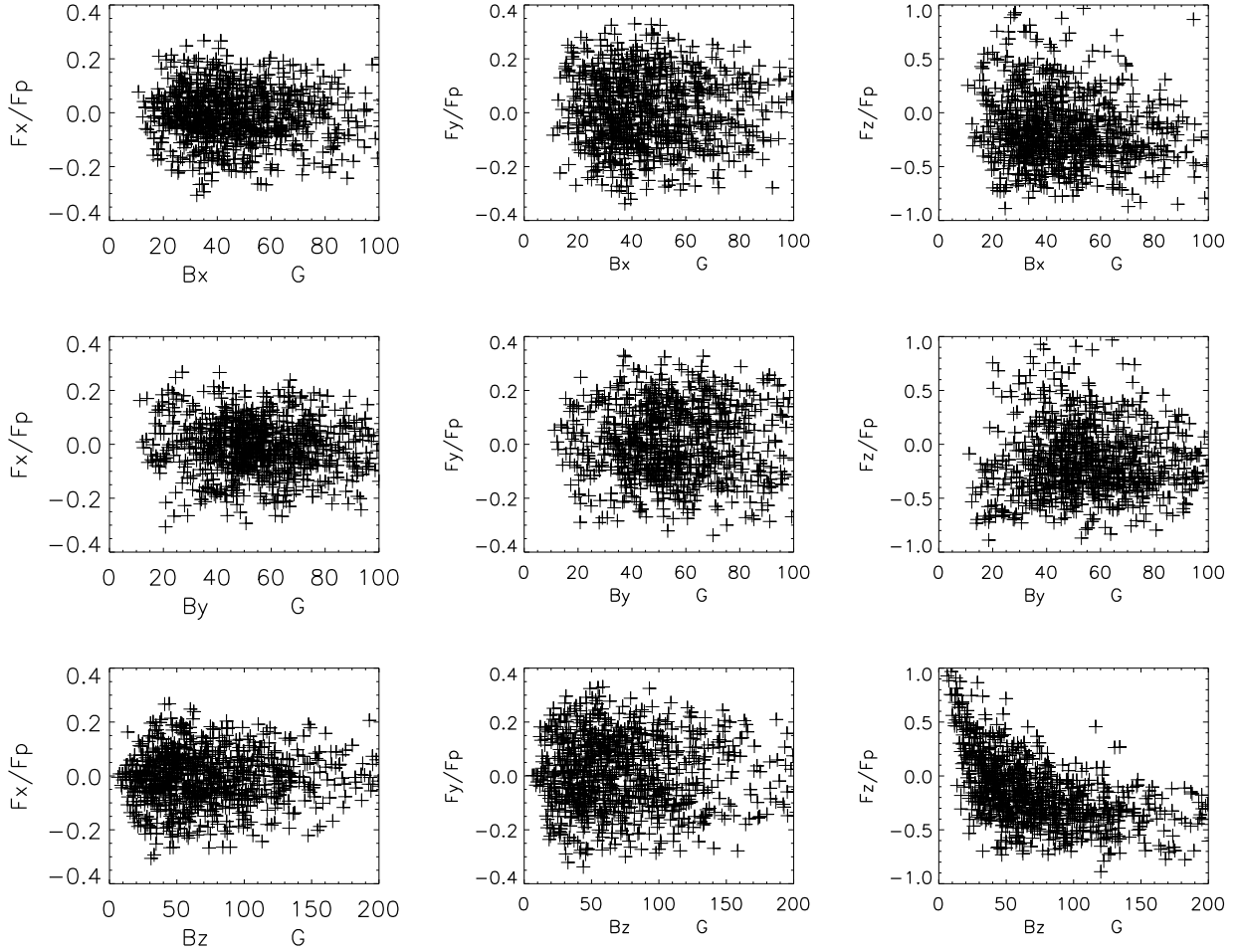


Fig. 2.— F_x/F_p , F_y/F_p and F_z/F_p vs B_x , B_y and B_z for the selected magnetograms. (CaseI)

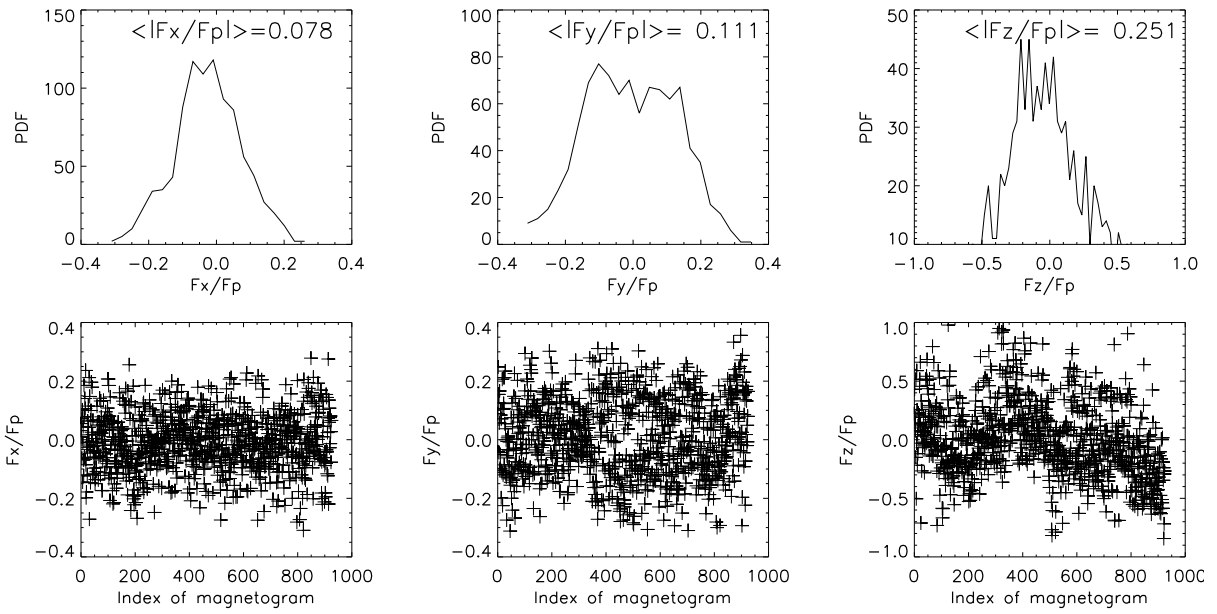


Fig. 3.— PDF and scatter diagrams of F_x/F_p , F_y/F_p and F_z/F_p for the selected magnetograms. The mean values of absolute F_x/F_p , F_y/F_p and F_z/F_p are plotted and indicated by $\langle |F_x/F_p| \rangle$, $\langle |F_y/F_p| \rangle$, $\langle |F_z/F_p| \rangle$, respectively. (CaseII)

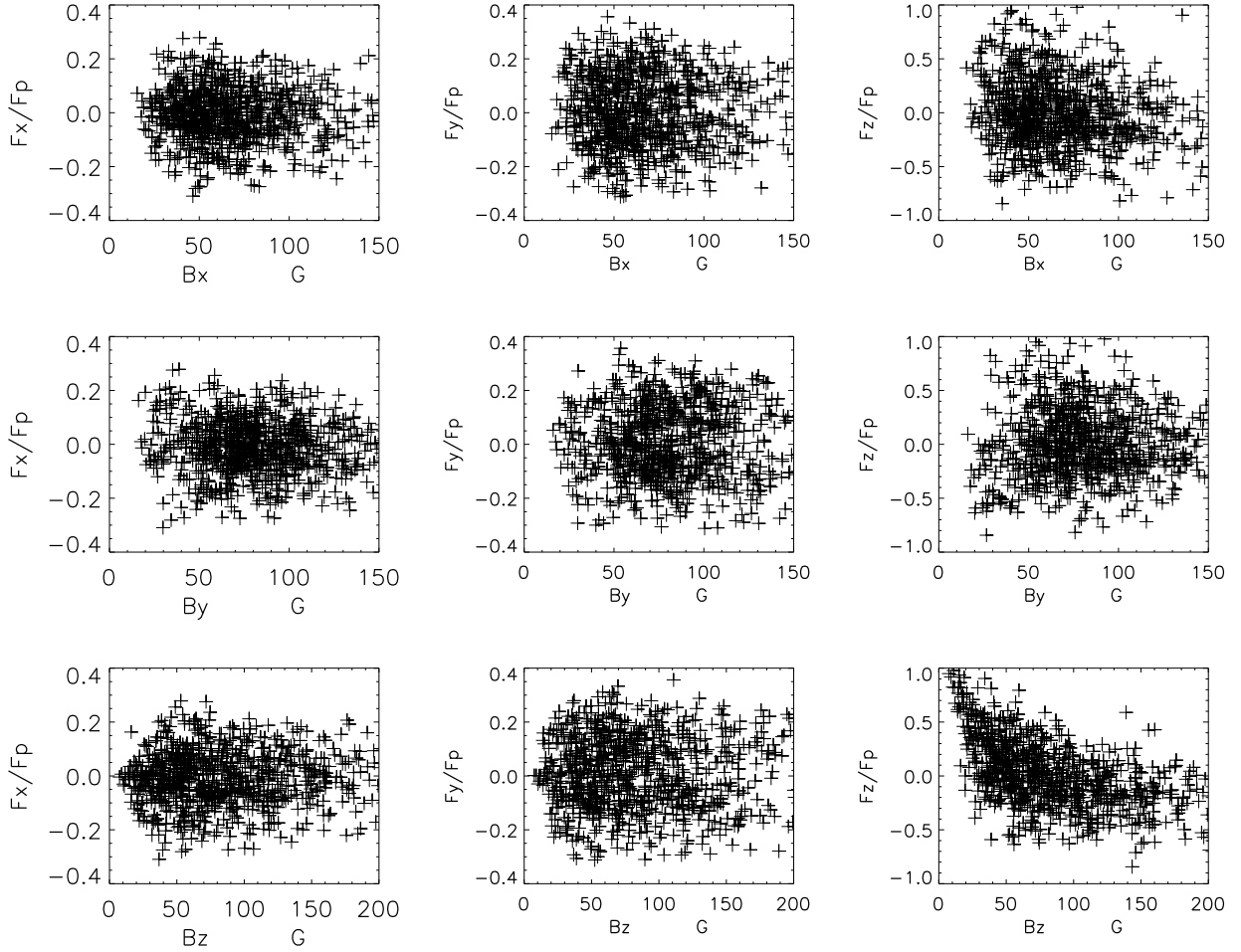


Fig. 4.— F_x/F_p , F_y/F_p and F_z/F_p vs B_x , B_y and B_z for the selected magnetograms. (CaseII)

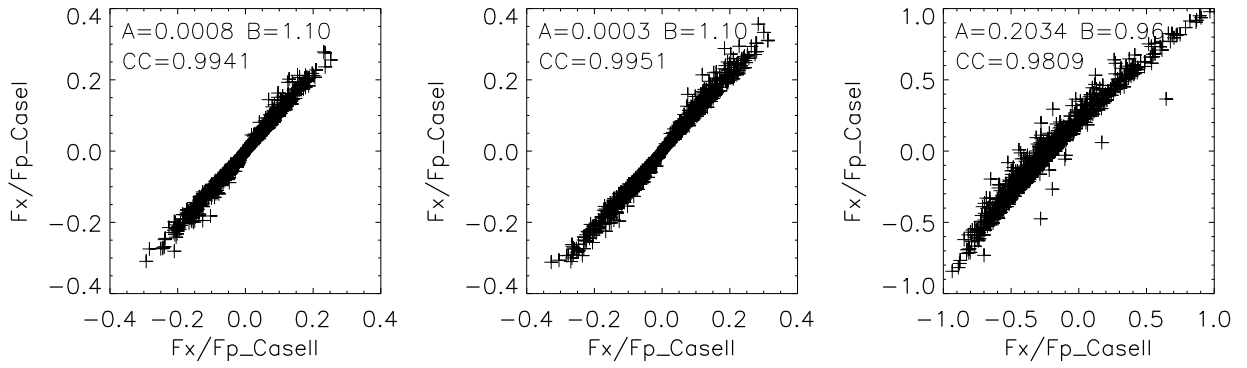


Fig. 5.— Scatter diagrams of F_x/F_p , F_y/F_p and F_z/F_p deduced from CaseI and CaseII, respectively, for the selected magnetograms.